ACS APPLIED MATERIALS & INTERFACES

Research Article

www.acsami.org

Multiple Phase Transition and Scaling Law for Poly(ethylene oxide)−Poly(propylene oxide)−Poly(ethylene oxide) Triblock Copolymer in Aqueous Solution

Sijun Liu and Lin Li*

School of Mechanical and Aerospace Engineering, Nanyang Technological University, 50 Nanyang Avenue, Singapore 639798, Singapore

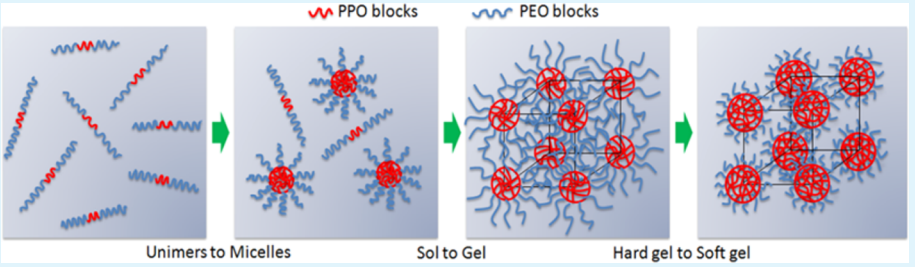

ABSTRACT: The multiple phase transition and the scaling behavior of a poly(ethylene oxide)−poly(propylene oxide)−poly(ethylene oxide) triblock copolymer (Pluronic F127, PEO_{100}−PPO_{65}−PEO_{100}) have been studied by micro-differential scanning calorimetry and rheology. The scaling behavior of the triblock copolymer was examined using the Winter−Chambon criterion to obtain the critical gel temperature T_{gel} and the scaling exponent n. n was found to decrease linearly with increasing copolymer concentration. A stable hard gel was formed, but the hard gel was transformed into a soft gel upon further heating. Increasing copolymer concentration led to the increase in the temperature of hard−soft gel transition, while the sol−gel transition temperature decreased with increasing copolymer concentration. A phase diagram has been determined, which is able to classify unimers, micelles, hard gel, and soft gel regions upon heating. In addition, the scaling relation of the plateau modulus G_e with copolymer concentration was also obtained as $G_e \approx c^{3.0}$ for both soft gel and hard gel.

KEYWORDS: *micelle, multiple phase transition, scaling law, gelation, rheology*

INTRODUCTION

In the past 20 years, considerable efforts have been made to understand the properties of poly(ethylene oxide)−poly(propylene oxide)−poly(ethylene oxide) triblock copolymers, PEO_m−PPO_n−PEO_m, where m and n represent number-average block lengths.[1−5] At low temperatures or low copolymer concentrations, the aqueous solution properties of PEO−PPO−PEO copolymers are now relatively clear. These copolymers exist as umimers because of the formation of hydrogen bonds between water molecules and copolymer chains. If PPO blocks and water are unable to form hydrogen bonds, a cage-like structure is considered to be formed in order to make them water soluble. Upon heating, PPO blocks gradually become insoluble due to the breakup of cage-like structures. An endothermic peak appears because the energy is required to destruct the cage-like structure. When the critical micellization temperature (CMT) or critical micellization concentration (CMC) is reached, the micelle structure consisting of a PPO core and PEO corona is formed. The size of micelles can be determined by many factors: molecular weight of copolymer, lengths of PPO and PEO blocks, and ratio of PPO to PEO blocks. Many studies have been performed on the micellar structure, size, and aggregation number for PEO−PPO−PEO triblock copolymers.[6−10]

The aqueous solution properties of PEO−PPO−PEO copolymers at high concentrations are very complicated. A crystalline lattice or an ordered structure is formed due to the arrangement of micelles, which is also usually called the gelation. Depending on the molecular architecture, molecular weight, concentration, and temperature, cubic (face-centered-cubic (fcc) or body-centered-cubic (bcc)), lamellar, and hexagonal crystalline structures have been reported.[11] For example, in the aqueous solution of F108 (PEO_{133}−PPO_{50}−PEO_{133}), fcc was reported.[11] Wanka et al. studied the influence of the ratio of PEO/PPO (m:n) on crystalline structure[12] and found that the copolymers with a shorter hydrophilic PEO block, i.e., m:$n \approx 0.25$, usually formed a hexagonal structure during the gelation, while a lamellar structure was formed for copolymers with m:$n \approx 0.15$. Upon imposing a shear flow to the gel, Eiser et al.[13] found that the highly aligned fcc crystals were transformed into bcc crystals. At a given copolymer concentration, transitions can also occur from one lattice to other lattice by varying temperature.[14−16] For example, in a P85 (PEO_{25}−PPO_{40}−PEO_{25}) aqueous solution,[10] micelles first were

Received: November 6, 2014
Accepted: January 7, 2015
Published: January 7, 2015

DOI: 10.1021/am507749w
ACS Appl. Mater. Interfaces 2015, 7, 2688−2697

packed into a cubic structure and then transformed into a phase of hexagonally packed rods at higher temperatures.[10]

Among various PEO−PPO−PEO copolymers, Pluronic F127 (PEO_{100}−PPO_{65}−PEO_{100}) is considered as the most prominent triblock copolymer in applications such as structure directing agents and drug delivery due to the various phase behaviors in water. At low F127 concentrations, heating leads to the dehydration of unimers, which results in aggregation and micellization.[17] At high F127 concentrations, Li et al.[18] observed that the aqueous solution of F127 exhibited a gelation at low temperature (22−30 °C) and a degelation at high temperature (50−60 °C). Mortensen et al.[19] reported that the aqueous solution of 20 wt % F127 formed fcc ordered micelles at 50 °C. In the research on the gelation kinetics of F127 upon heating, Meznarich et al.[20] observed the second endothermic peak in the calorimetric curve, which corresponded to the order of the micelles. Wanka et al.[12] also observed this phenomenon for a F127 aqueous solution but considered it to be attributed to the dehydration of PPO blocks. All of these research works indicated that there is a complexity in the phase transitions of F127 in aqueous solution upon heating at high concentrations.

On the other hand, the rheological properties of aqueous solutions of PEO−PPO−PEO copolymers have been investigated. When copolymer molecules are present as unimers or individual micelles, the solutions are Newtonian fluids. When PEO−PPO−PEO micelles are connected, the solutions will become gels, where the loss modulus G'' of the gels can be as high as the storage modulus G', which displays a very different rheological behavior from other hydrogels such as methylcellulose.[21] A number of experiments have shown that the PEO−PPO−PEO gels with various crystalline structures possess different viscoelastic properties. From the study of F68 (PEO_{76}−PPO_{29}−PEO_{76}) and F108 copolymers, Eiser et al.[13] found that the ordered micelles with a bcc structure in an F68 solution did not have any measurable yield stress, but in the same study, the ordered micelles with an fcc structure in a F108 solution could have a yield stress due to the restriction of movement of defects in the grain boundary.

However, the rheological studies for the aqueous solution of PEO−PPO−PEO have not covered the sol−gel transition in depth so far. To the best of our knowledge, there have not been direct reports dealing with the critical gelling behavior and rheological scaling laws for F127 in water upon heating. Therefore, in this report, we have systematically investigated the phase transitions and rheological properties of F127 aqueous solution using micro-differential scanning calorimetry and rheology. The rheological scaling laws were examined and discussed for the first time for understanding of the gelation and the relationship of viscoelastic properties with the features of its microstructures. A schematic diagram has been proposed for multiple phase transitions in concentrated aqueous solutions of F127 upon heating.

EXPERIMENTAL SECTION

Materials and Solution Preparation. The poly(ethylene oxide)−poly(propylene oxide)−poly(ethylene oxide) triblock copolymer, F127, donated as PEO_{100}−PPO_{65}−PEO_{100}, was kindly provided by BASF Corp. Its molecular weight and ethylene oxide content are 12600 g/mol and 70 wt %, respectively. The melting point of F127 is 65 °C, and it is in the form of flakes at ambient temperature. F127 was dried and kept in a desiccator before use.

The preparation of F127 aqueous solutions with copolymer concentrations ranging from 15 to 30 wt % is similar to that described in ref 22.

Micro-Differential Scanning Calorimetry. Calorimetry is an important method that directly determines the enthalpy and is also a primary technique to be used to establish the connection between material property and temperature. In contrast to conventional DSC that is suitable for solid samples, micro-DSC is suitable for liquid solution samples, especially aqueous solutions, and it can detect a tiny heat change (microcalories) during heating or cooling. The use of micro-DSC can be simply found from the literature. In this study, the thermal behavior of F127 aqueous solutions was determined by a micro-DSC (VP-DSC microcalorimeter, Microcal Inc.). 0.516 mL of an F127 aqueous solution was injected into the sample cell, while the same volume of deionized water was injected into the reference cell. The scan rate of 1 °C/min was adopted. To make sure there was no contamination, the sample cell was cleaned by the continuous deionized water after each cycle was completed.

Rheological Measurement. A rotational rheometer (DHR, TA Instruments, USA), with a parallel plate of 40 mm diameter and a Peltier temperature control, was employed to investigate the rheological properties of F127 aqueous solutions. The sample for rheological measurements was loaded directly from a solution bottle kept in a refrigerator to the rheometer using a pipette. Strain sweeps with various frequencies were carried out in the range of 0.1−100% to determine the linear viscoelastic range. A small amount of low-viscosity silicone oil was placed on the peripheral surface between the upper and lower plates to prevent evaporation of water. Two rheological measurements were performed for various F127 concentrations: (1) temperature ramps at a heating rate of 1 °C/min with the strain of 1.0% and the frequency of 1 Hz to study the transitions from unimers to micelles and then micelles to gels over a temperature range of 10−90 °C, and (2) frequency sweeps at different temperatures in the angular frequency 0.1−100 rad/s and at a constant strain 1.0%.

RESULTS AND DISCUSSION

Multiple Phase Transitions. Figure 1 shows the calorimetric thermograms of F127 aqueous solutions with various copolymer concentrations from 15 to 30 wt % at a scanning rate of 1 °C/min. Because of the dehydration, a sharp endothermic peak was observed during heating. PPO blocks become insoluble and the micellization of F127 begins. The onset temperature of micellization, which is usually defined as

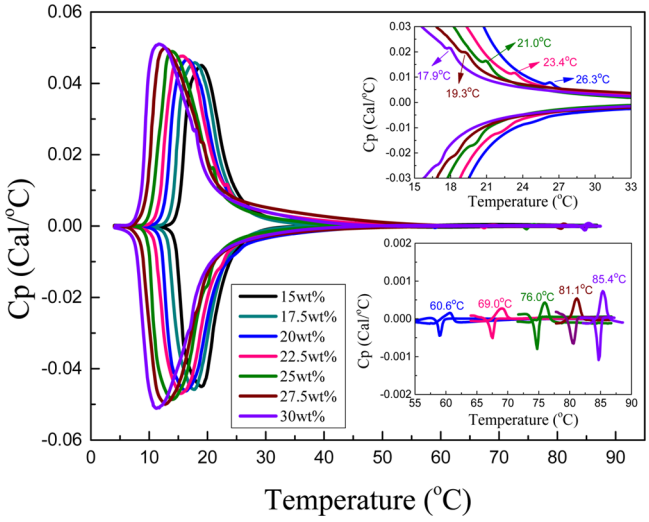

Figure 1. Thermal behavior of F127 aqueous solutions with various copolymer concentrations at a rate of heating and cooling of 1 °C/min. The second transition peak from 15 to 33 °C and the third transition peak from 55 to 90 °C are enlarged in the insets and denoted as T_{mg} and T_{hs} respectively.

DOI: 10.1021/am507749w
ACS Appl. Mater. Interfaces 2015, 7, 2688−2697

the critical micellization temperature (CMT), decreases with increasing F127 concentration, while the height of peak increases with F127 concentration. In the subsequent cooling process, the corresponding exothermic peaks appear. Along the baseline, the endothermic and exothermic curves display the mirror relationship for each concentration.

For aqueous solutions of 15 and 17.5 wt % F127, no peaks appear in the temperature range of 5−90−5 °C except for micellization and demicellization. When F127 concentration increases to 20 wt % or higher, two small endothermic peaks appear during heating, and then the corresponding exothermic peaks are observed in the subsequent cooling process. The enlarged thermal diagrams are inserted into Figure 1. It is believed that the changes of some structure should be associated with these small peaks during the processes of heating and cooling. For aqueous solutions of F108,[22] it was found that a second transition peak appears at the offset temperature of micellization and the authors attributed the transition peak to the gelation of F108. Armstrong et al.[23] found that there was a second transition in the range of 60−70 °C for a dilute solution of P235 (PEO_{27}−PPO_{39}−PEO_{27}) added with sodium chloride, and they explained the second transition to be due to the transition of sphere micelles to rod-like micelles. For an aqueous solution of F127, the formation of different crystalline structures has been studied, which has been described in the introduction. Recently, Pham Trong[24] studied the mechanisms of micellization and gelation of F127 using micro-DSC and found a very small second endothermic peak corresponding to ordering of micelles, whereas the scanning calorimetry did not show any endothermic peaks at higher temperatures for the concentrated F127 solution. Figure 1 shows that there is a second transition peak from 15 to 30 °C and a third transition peak from 55 to 90 °C for the F127 concentrations of 20−30 wt %, and the second transition temperature decreases and the third transition temperature increases with increasing F127 concentration. Thus, it is inferred that the second transition peak should be ascribed to the F127 gelation. The micellization is a prerequisite for the gelation. For the third transition peak, it should be related to the hard gel−soft gel transition, which will be discussed later. Because the heats for the sol−gel and hard gel−soft gel transitions are much smaller compared to the heat of micellization, they are nearly athermic. In this study, the second and third transition temperatures are denoted as T_{mg} and T_{hs}, respectively.

To verify the above inference, rheological temperature ramps with the same heating rate as micro-DSC was carried out. The dependence of storage modulus G', loss modulus G'', and relative thermal capacity C_p on temperature for 15, 20, and 25 wt % F127 aqueous solutions are shown in parts a, b, and c of Figure 2, respectively. For the 15 wt % F127 aqueous solution, Figure 2a could be divided into three regions. In region 1, when the temperature is below its CMT of 13.2 °C, polymer chains exist as unimers, the constant G' and a decrease in G'' with temperature are observed, and the solution shows the characteristic of a Newtonian fluid. The micellization begins at CMT and reaches to the maximum value at the peak temperature T_p, 19.0 °C. In the temperature range between CMT and T_p, unimers and micelles coexist in water, whereas G'' decreases continuously due to the dehydration of unimers and the solution is still dominated by unimers. The similar phenomenon was found for the branched PEO−PPO−PEO.[25,26] In region 2, with further increase in temperature,

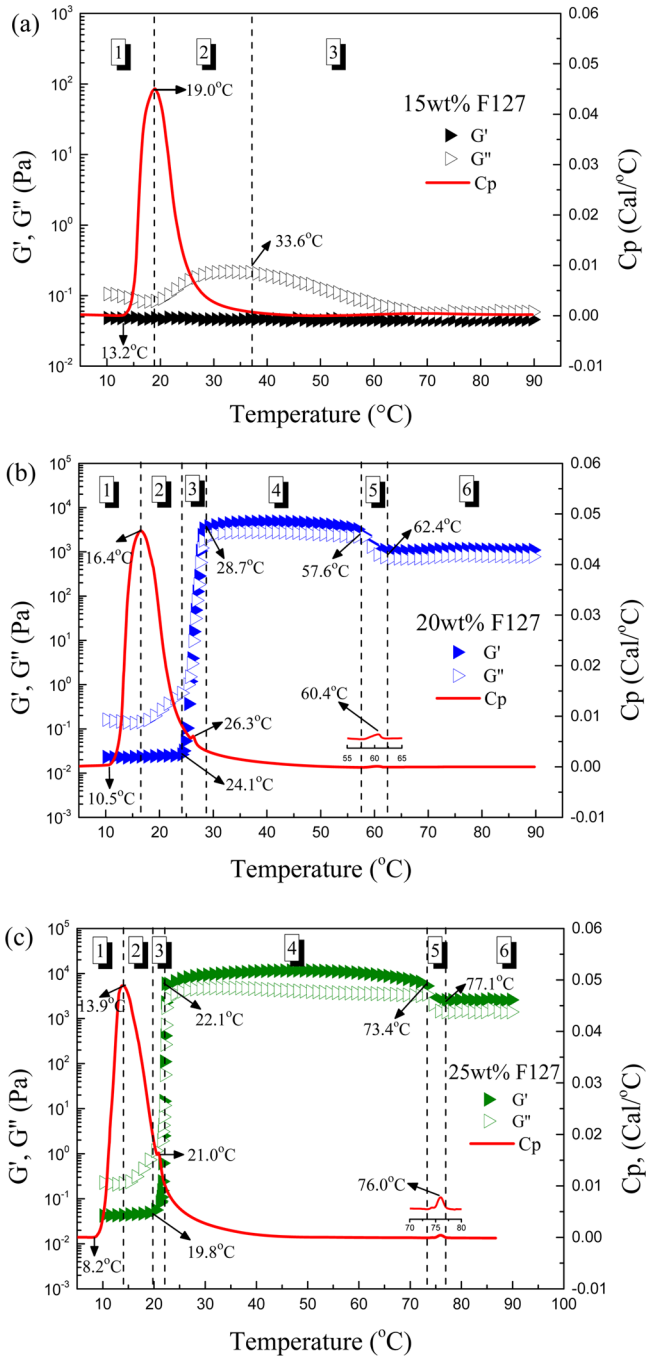

Figure 2. Dependence of C_p, G', and G'' on temperature for F127 aqueous solutions at the various concentrations: (a) 15 wt %, (b) 20 wt %, and (c) 25 wt %, respectively. Oscillatory frequency and shear strain amplitude were 1 Hz and 1%, and the heating rate was 1 °C/min.

many more micelles are formed. G'' slightly increases while G' keeps almost constant. A similar evolution has already been observed for the kinematic viscosity of the aqueous solution of a branched PEO−PPO−PEO.[27] At 33.6 °C, which is very close to the offset temperature T_{off}, indicating the end of micellization, G'' reaches to the maximum (0.22 Pa) and almost all chains of F127 exist in the micelles. In region 3, G'' decreases with increasing temperature, and the system shows a liquid state. It can be concluded from the above results that the dehydrated micelles are unable to contact each other to form an

DOI: 10.1021/am507749w
ACS Appl. Mater. Interfaces 2015, 7, 2688−2697

ordered structure because of the low micelle density in the aqueous solution of 15 wt % F127.

Figure 2b shows the effect of temperature on C_p, G' and G'' for the 20 wt % F127 aqueous solution, which could be divided into six regions. In region 1, G'' decreases and reaches the minimum at T_p for the same reason as for the 15 wt % F127 solution. In region 2, the formation of many more micelles results in a slow increase in G''. G' and G'' increase sharply in region 3, which responds to the gelation because the micelles begin to contact each other to form an ordered structure that contributes to the high modulus. Meanwhile, it is apparent that the second transition peak temperature of 26.3 °C in the micro-DSC curve locates in region 3, which further proves that the second transition peak should be attributed to the gelation even if the enthalpy is at most a few percent of that of micellization. The crossover point temperature of G' and G'' is tranditonally defined as the gel point, but this definition has a frequency dependence and will be discussed later. In region 4, G' is larger than G'', and both moduli reach to their own plateau, so the system shows a solid-like behavior. As the temperature increases to 57.6 °C, G' and G'' decrease and the system falls to the second plateau after 62.4 °C. Here we denoted this transition region from 57.6 to 62.4 °C as region 5. In this region, G' and G'' almost parallel decrease, while the solution is still elastic because G' is larger than G'', which is different from a gel−sol transition. Meanwhile, it is interestingly noted that the third transition peak in the micro-DSC curve lies just in region 5. In fact, temperature shows an important influence on the formation of ordered micelles and the stability of a gel structure. In the low temperature region (regions 1 and 2), the increase in temperature results in the increases in the size and number of micelles but the decrease in intermicellar distance. After the sol−gel transition, the concentration of micelles is not changed by temperature because almost all of polymer chains already exist in the micelles. With further increasing temperature, the decrease in PEO block's solubility may cause a part of PEO blocks to be merged into the cores of micelles, which increases the size of micellar cores and reduces the corona overlapping degree, leading to the decrease in entanglement density of PEO blocks in the overlapped corona and then the drop of modulus. The similar experimental phenomena have also been observed for aqueous solutions of P85[28] and P105 (PEO_{37}−PPO_{56}−PEO_{37})[29] copolymers. In region 6, a high temperature gel is formed, which has the lower modulus compared to the low temperature gel. Here, we define the high temperature gel as the soft gel and the low temperature gel as the hard gel because the elastic modulus of the low temperature gel is more than 1 order of magnitude larger than the high temperature gel.

The 25 wt % F127 solution is shown in Figure 2c, which is also divided into six regions. With increasing temperature, micellization begins at 8.2 °C and the rate of micellization reaches maximum at T_p of 13.9 °C. The formation of massive micelles results in the increase of G''. G' and G'' increase sharply, and the gelation is observed from 19.8 to 22.1 °C, followed by the appearance of a hard gel in region 4 until 73.4 °C. Then the modulus of the hard gel decreases in the vicinity of 73.4 °C because of the decrease in the entanglement density, which was induced by the reduced solubility of PEO block at high temperatures. As a result, a soft gel was formed after 77.1 °C. The second and third transition peaks in the micro-DSC curves further prove the transitions of sol−gel and hard gel−soft gel. Compared to the 20 wt % F127 solution, it is noted that the temperature regions for the sol−gel transition and the transition of hard gel−soft gel decrease from ΔT = 28.7−24.1 = 4.6 (°C) to ΔT = 22.1−19.8 = 2.3 (°C) and from ΔT = 62.4−57.6 = 4.8 (°C) to ΔT = 77.1−73.4 = 3.7 (°C), respectively, indicating that the rates of the gelation and the transition of hard gel−soft gel increase with increasing F127 concentration.

From the above results, we may conclude that the micelles could not contact each other to form a gel at low F127 concentrations (below 20 wt %). When F127 concentration increases to 20 wt % or higher, spherical micelles of F127 in aqueous solution are packed into an ordered structure and then a gel is formed. The so-formed gels are unstable during heating because the solubility of PEO blocks decreases as temperature increases, which leads to the increase of core size of micelles due to the merging of a part of PEO blocks into micellar cores and the decrease of overlapping degree of micellar corona.

Because rheology is sensitive to a change in microstructure, we are able to correlate viscoelastic properties of a material with its microstructure. Although it was reported in the literature that the formation of ordered micellar structures from micelles is an athermal process,[22,30,31] our micro-DSC results show that the two tiny endothermic peaks beyond the micellization corresponded to the transitions of sol−gel and hard gel−soft gel, indicating a multiple phase transition taking place in the concentrated F127 aqueous solutions during heating.

The effect of temperature on G' and G'' for F127 aqueous solutions with copolymer concentrations from 20 to 30 wt % is shown in Figure 3. The rheological data for the aqueous

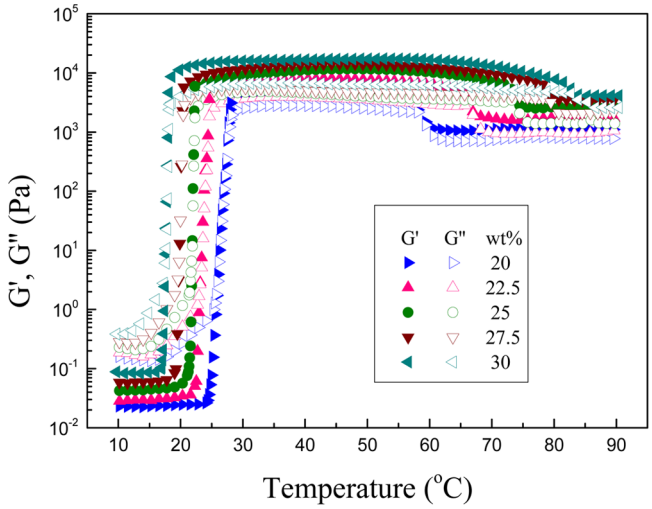

Figure 3. Dependence of G' and G'' on temperature for F127 aqueous solutions with copolymer concentrations from 20 to 30 wt %, and an oscillatory frequency 1 Hz and a shear strain amplitude 1% were applied.

solutions of F127 below 20 wt % are not shown in Figure 3 because these solutions could not form gels. Many characteristic features can be observed from the rheological curves. For example: (1) increasing F127 concentration results in the decrease in the gel temperature. This is because that the number density and volume fraction of micelles increase with F127 concentration, so that the distance between micelles decreases, leading to an earlier formation of a micellar network. (2) In both hard gel and soft gel, the heights of G' and G'' increase with F127 concentration due to the densely packed micelles, which are connected through intermicellar entangle-

DOI: 10.1021/am507749w
ACS Appl. Mater. Interfaces 2015, 7, 2688−2697

ment of PEO blocks, contribute to the viscoelasticity significantly. (3) The temperature of the hard gel−soft gel transition increases as F127 concentration increases due to the increased intermicellar interaction. The temperature window for the hard gel becomes wider with increasing F127 concentration. From Figure 3, it is apparent that the different phase transitions have a strong dependence on copolymer concentration.

The dynamic frequency sweep for the 20 wt % F127 solution is shown in Figure 4, which further demonstrates a profound

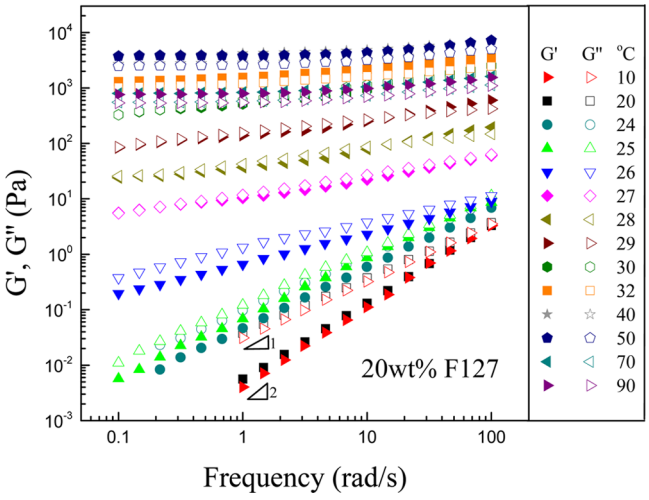

Figure 4. G′ and G″ as a function of angular frequency for the aqueous solution of 20 wt % F127 at different temperatures.

change in dynamic viscoelasticity upon heating. In the unimer zone, for example, at 10 °C, G″ is higher than G′, and both G′ and G″ obey the scaling behavior of $G' \sim \omega^2$ and $G'' \sim \omega^1$ in the terminal frequency region, which indicates that the solution is a Newtonian fluid. At 20 °C at which unimers and micelles coexist, a notable deviation from the terminal behavior can be observed. Shchipunov et al.[32] thought that this phenomenon should be ascribed to the presence of the largest micelles in aqueous solution. At 27 °C, both G′ and G″ are higher than those at 26 °C in the whole frequency region and G′ is almost equal to G″, indicating that micelles have contacted each other and the system is approaching to a gel state. The gap between the curves for 26 and 27 °C is striking. When the temperature increases to 32 °C, G′ becomes higher than G″, which is a typical solid-like behavior. At 40 °C, both moduli reach to the maximum values. However, they drop at 70 °C due to the transformation of the hard gel into the soft gel but keep almost constant at 90 °C. The rheological frequency sweep results (Figure 4) are consistent with the temperature ramp results (Figure 3), further verifying that the transformation of the hard gel to the soft gel is frequency-independent. The frequency dependence of G′ and G″ on other F127 concentrations is similar to that observed in Figure 4 (data not shown here).

As shown in Figure 5, we propose a mechanism for the multiple phase transitions of concentrated F127 aqueous solutions upon heating. At low temperatures, the copolymer exists as unimers, so the solution is a Newtonian fluid. PPO blocks start to dehydrate upon heating, and the micellization takes place. Aggregates of PPO blocks form the cores of micelles, which are surrounded by the hydrated PEO blocks. The heat of micellization, which was used for dehydration of PPO blocks or destruction of a cage-like water structure, was detected by micro-DSC. With further increasing temperature, the size and number of micelles increase and the intermicellar distance decreases. At a given temperature and a given copolymer concentration, the micelles are packed into an ordered structure, leading to the gelation. The gelation temperature decreases with increasing F127 concentration. The second endothermic peaks are very consistent with the observations by the rheological measurements, although the heat was too small. At higher temperatures, the merging of a part of PEO blocks into micellar cores due to the decrease of the solubility of PEO blocks increases the size of micellar cores and reduces the degree of overlapping of micellar coronas, which leads to decrease in the entanglement density of PEO blocks as well as the transition of hard gel−soft gel. Therefore, it is apparent that there are three phase transitions (unimer−micelle, sol−gel, and hard gel−soft gel) for 20 wt % and higher concentrations of F127 aqueous solutions upon heating and each of these phase transitions shows a strong dependence on F127 concentration.

Determination of Critical Gel Temperature. The critical temperature for the gelation at a given copolymer concentration is important in practical applications such as controlled drug delivery and injectable biomaterial.[33,34] Traditionally, the crossover of G′ and G″ was used as the gel point. Because of the frequency dependence, the crossover of G′ and G″ does not always occur. Winter and Chambon[35] proposed a criterion (known as Winter−Chambon criterion) to determine the chemical gels with a power law behavior at the gel point, $G'(\omega) = G''(\omega) \sim \omega^{1/2}$. Subsequently, this equation was generalized into $G'(\omega) \sim G''(\omega) \sim \omega^n$ $(0 < n < 1)$ at a sufficiently low frequency for other gel systems. Because a gelation variable loses its dependency on frequency, this method shows an excellence for determination of the gel point, such as PVC/

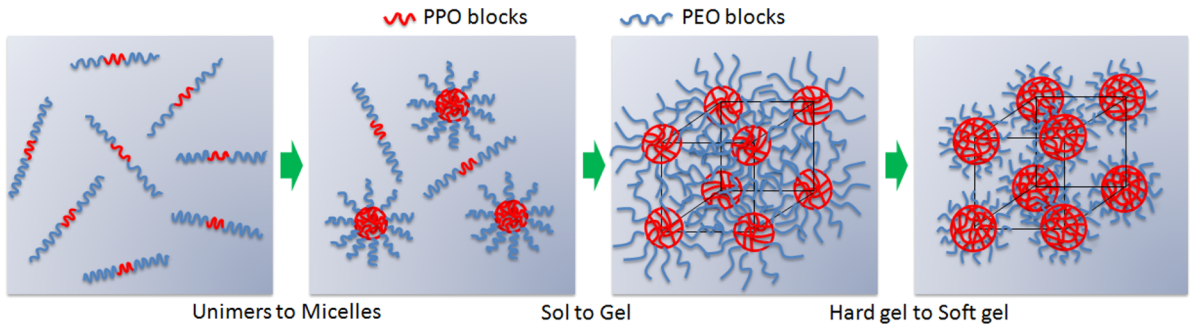

Figure 5. Schematic diagram for multiple phase transitions in concentrated aqueous solutions of F127 in a heating process.

DOI: 10.1021/am507749w
ACS Appl. Mater. Interfaces 2015, 7, 2688−2697

DOP systems,[36,37] where PVC stands for poly(vinyl chloride) and DOP is bis(2-ethylhexyl) phthalate. However, whether the gel point can be measured by this method for gel formation induced by micellar packing has not been reported for a PEO−PPO−PEO aqueous system.

From the frequency sweep results for the 20 wt % F127 solution (Figure 4), a liquid-like state was obtained at temperatures below 26 °C and a gel-like state was obtained at 27 °C and above. Thus, the gelation should take place in between 26 and 27 °C. Figure 6 shows the dependence of tan δ

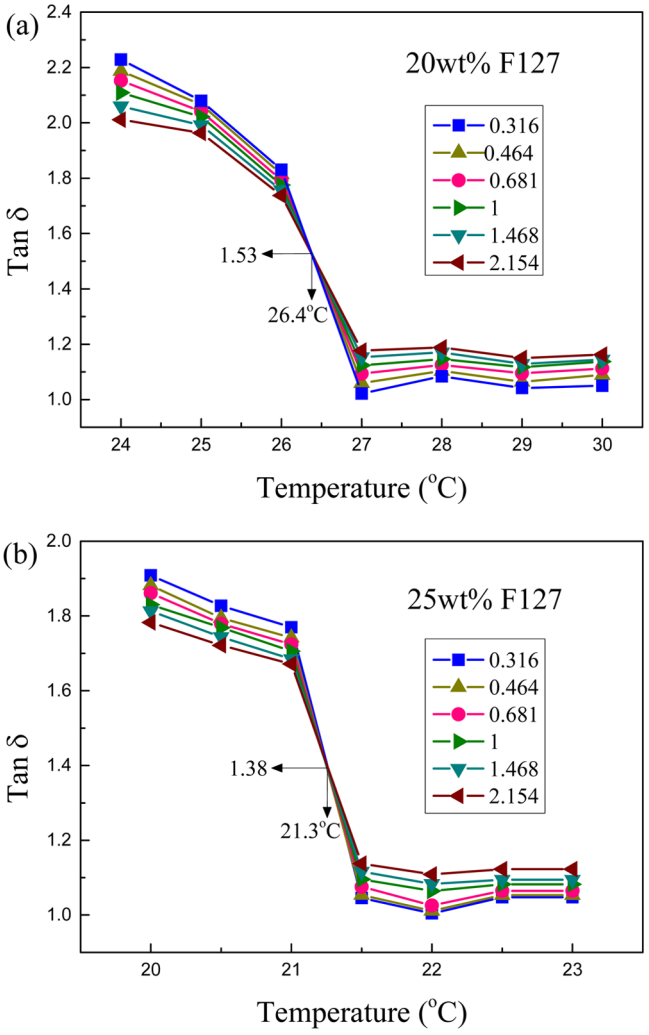

Figure 6. Dependence of loss tangent, tan δ, on temperature at different angular frequencies in rad/s as indicated for aqueous solutions of (a) 20 wt % and (b) 25 wt % F127.

on temperature at different angular frequencies for aqueous solutions of 20 and 25 wt % F127. All curves pass through the common point at 26.4 °C for 20 wt % F127 and at 21.3 °C for 25 wt % F127. These points are defined as the critical gel temperatures, T_{gel}. Meanwhile, we can see that the second transition temperatures 26.3 °C for 20 wt % F127 and 21.0 °C for 25 wt % F127 found in the micro-DSC curves are very close to the critical gel temperatures, further suggesting that the second transition peaks should be related to the gelation.

Phase Diagram. The phase diagram of F127 in aqueous solution is shown in Figure 7, and the phase boundaries were determined by micro-DSC and the Winter−Chambon

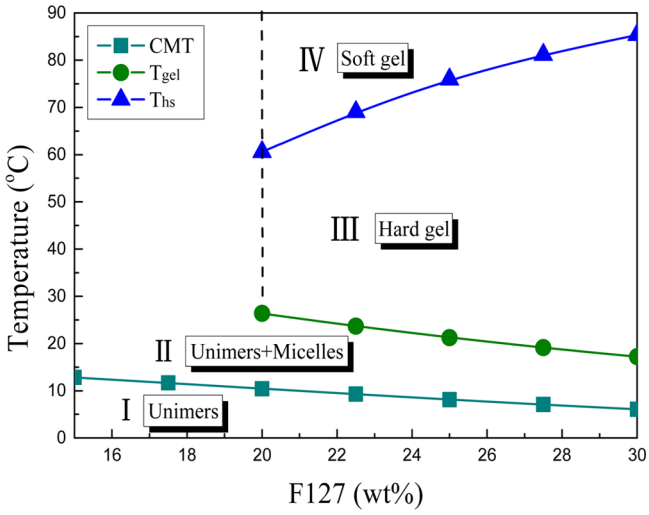

Figure 7. Phase diagram of F127 in aqueous solution, which was obtained by micro-DSC and rheology. For F127 concentrations less than 20 wt %, F127 is unable to form a gel, so F127 exists as unimers and/or micelles. Four regions could be defined: I, unimers; II, unimers and micelles; III, hard gel; IV, soft gel, where the dash line roughly indicates the boundary between the micelle region and the hard gel and soft gel region.

criterion. Although the phase behavior of F127 in the thermodynamic equilibrium state could not be reflected by this phase diagram due to the fact that CMT and T_{hs} are dependent on heating rate, this kind of phase diagram is useful to describe the kinetic phase behavior in the concentration range used in this study. The phase diagram is divided into four regions. In region I, the copolymer exists as individual molecular chains (unimers) below CMT due to the excellent solubility of PEO and PPO blocks at low temperature. In region II, when the temperature or concentration is high, unimers self-associate into micelles that coexist in water with unimers. CMT decreases monotonously with concentration, which is consistent with those observed by Meznarich.[20] In region III, where copolymer concentration is high (≥20 wt %), a solid-like gel is formed above T_{gel}. In region IV, the solubility of PEO blocks in coronas decreases at higher temperatures and a part of PEO blocks is merged into micellar cores, which reduces the overlapping degree of micellar coronas and induces the hard gel to transform into the soft gel. Because T_{gel} decreases and T_{hs} increases with increasing copolymer concentration, the area for the hard gel broadens. The phase diagram clearly demonstrates the phase changes of a F127 aqueous solution with copolymer concentration and temperature.

Scaling Law. The formation and properties of gels have been extensively studied by experimental and theoretical methods based on the scaling law. To examine and explain rheological properties in the vicinity of the gel point, the widely used scaling law has been proposed[35,38,39]

$$G''(\omega)/G'(\omega) = \tan\delta = \tan(n\pi/2) \quad (1)$$

which was inferred by the shear relaxation modulus $G(t)$ at the gel point

$$G(t) = S_g t^{-n} \quad (2)$$

where S_g is denoted as the gel strength and n is named as the critical or scaling exponent. At the gel point, a similar equation can also be applied for G' and G''

DOI: 10.1021/am507749w
ACS Appl. Mater. Interfaces 2015, 7, 2688−2697

$$G'(\omega) = G''(\omega)/\tan(n\pi/2) = S_g\omega^n\Gamma(1-n)\cos(n\pi/2) \quad (3)$$

where $\Gamma(1-n)$ is the Gamma function. It is easy to calculate S_g using eq 3 with n and $G'(\omega)$ or $G''(\omega)$.

Using eq 1, we obtained n = 0.63, 0.61, 0.60, 0.58, and 0.56 for 20, 22.5, 25, 27.5, and 30 wt % F127 from the critical gel temperatures, respectively, and the results are shown in Figure 8. Thus, n was obtained as a linear function of F127 concentration:

$$n = 0.766 - 0.0068c \quad (4)$$

where c is F127 concentration over the concentraion range.

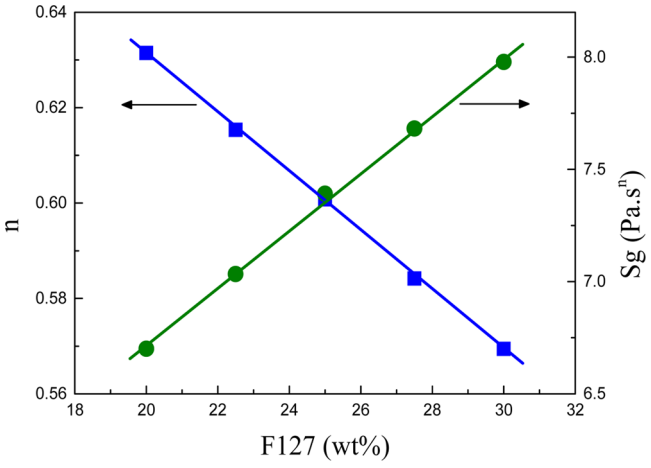

Figure 8. Relationships of the scaling exponent n and gel strengthen S_g with F127 concentration.

Much works have shown that the values of n are dependent on various gelling systems. n was reported to be between 0.2 and 0.3 for the chemical gels.[40,41] For physical gels, n is relatively high. For example, for PVC/DOP gels formed by small crystallite domains, n was reported to be 0.75.[36,37] In poly(vinyl alcohol) (PVA) physical gels formed by hydrogen bonding, n was found to be 0.65.[42] The sol−gel transition induced by electrostatic interaction in the mixture consisting of oppositely charged polyelectrolyte (quaternized hydroxyethylcellulose ethoxylate, QHEC) and nanocrystalline cellulose (NCC), n changed from 0.785 to 0.773 at different concentrations of QHEC.[43] All of these results indicate that the various n values may be derived from the different gelation mechinisms in the physical gelling systems. The gelation theories depending on the model assumption such as Rouse behavior and Zimm behavior predict that n is located between $^2/_3$ and 1,[39] which is consistent with the experimental results. However, there has not been any detailed study in the literature about the relationship of n with the gelation and gel microstructures that are induced by micellar packing.

Figure 6 has shown that the critical gel temperature decreases with increasing F127 concentration, indicating that it is easier for the micelles to be connected at a higher copolymer concentration. The dependence of critical relaxation exponent, n, on F127 concentration is shown in Figure 8. n decreases with increasing F127 concentration. The various n at different F127 concentrations can be understood from the intermicellar interaction. With a higher F127 concentration, a larger number of micelles will be formed which will result in a denser micellar network with a higher entanglement density of PEO blocks. Hence, the decrease of n should be attributed to the increase in the entanglement density of PEO blocks. Such a phenomenon is similar to chemical gels in which the increase in the cross-linking density results in a decrease of n.[44]

The physical properties of gels at the critical gel point can also be described by S_g. We are able to take the advantage of eq 3 to determine S_g when n is known for a given F127 aqueous solution. The examples of this kind of plot are illustrated in Figure 9 for 20 and 25 wt % F127 aqueous solutions. The

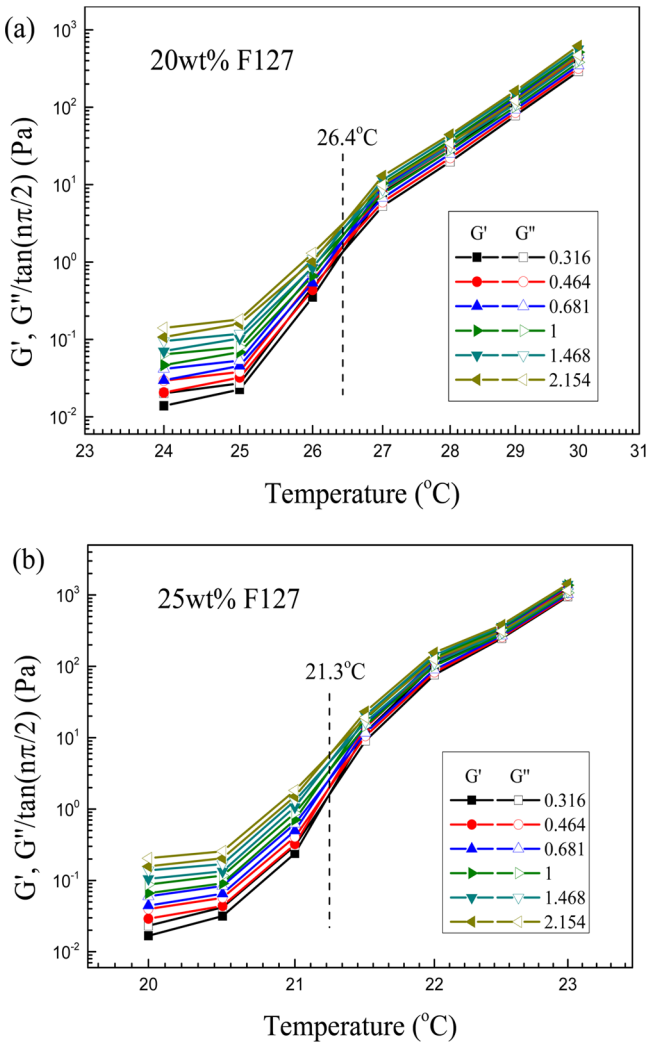

Figure 9. G' and $G''/\tan(n\pi/2)$ versus temperature for aqueous solutions of (a) 20 wt % and (b) 25 wt % F127 with frequency varying from 0.316 to 2.154 rad/s. The critical gel temperature is indicated by the dotted line.

crossover points appear quite well at 26.4 and 21.3 °C for 20 and 25 wt % F127 concentrations, which are consistent with the results obtained by the Winter−Chambon criterion. Thus, we obtained S_g using eq 3, which was plotted against F127 concentration in Figure 8. S_g increases with increasing F127 concentration, and a linear relationship of S_g with F127 concentration was obtained. This indicates that a higher F127 concentration induces much more micelles to result in a higher entanglement density in the micellar corona. That is to say, S_g is related to the total mass of copolymer and the increase in the entanglement density of PEO blocks results in an increase of S_g at the gel point.

DOI: 10.1021/am507749w
ACS Appl. Mater. Interfaces 2015, 7, 2688−2697

From the rheological temperature ramp results shown in Figure 3, both G' and G'' increase sharply at the gel point and then they reach to the gel plateau with further increasing temperature. Thus, we are able to obtain the plateau values of G', denoted as G_e. One scaling law was extensively applied to establish the relationships of G_e with polymer concentration beyond the sol−gel transition[38,45]

$$G_e = k\varepsilon^z \text{for } p > p_g \quad (5)$$

where k and z are the front constant and the scaling exponent, respectively, and ε [$= (p - p_g)/p_g$] is defined as the relative distance from a gel variable (p) to the sol−gel transition point (p_g). From G' curves in Figure 3, we have been able to define two gel states: the low temperature hard gel and the high temperature soft gel when F127 concentration is greater than 20 wt %. To examine the validity of the scaling law for G_e, we defined G' at 90 and 40 °C as G_e in the soft gel region and the hard gel region, respectively. Note that we directly used F127 concentration c instead of the relative distance ε because we have not known the critical gel concentration. This treatment does not change the basic feature of the scaling law.

Figure 10 shows the dependence of G_e on F127 concentration. It is observed that the decrease in PEO block's solubility at higher temperature reduces the degree of overlapping of micellar coronas and the intermicellar interaction. The PEO blocks in micellar coronas are believed to be entangled during the sol−gel transition. The entanglement density of PEO blocks in the micellar coronas determines the value of the plateau modulus. Thus, G_e of the high temperature gel is lower than that of the low temperature gel at a given F127 concentration. Moreover, like the critical gel strength S_g, G_e increases with increasing copolymer concentration. A linear fitting was carried out in order to obtain the scaling exponent z, which gave the following relations

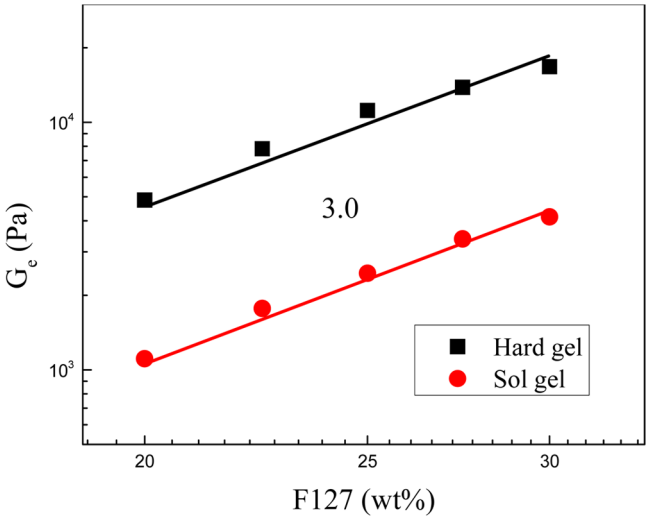

Figure 10. Dependence of the plateau modulus G_e on F127 concentration for soft gel and hard gel.

$$G_e = 0.573c^{3.0} \text{ for hard gel} \quad (6)$$

$$G_e = 0.066c^{3.0} \text{ for soft gel} \quad (7)$$

The correlation coefficients were higher than 0.99, indicating a good fitting. The various values of n have been predicted based on the different theories. For example, de Gennes predicted $z = 1.9$ according to the percolation model.[46] According to the entanglement theory, Liu predicted $z = 2.0$.[47] The mean-field theory predicted $z = 3.0$.[48] The experimental results show that the values of z are also dependent on the gel systems. For example, $z = 2.0-2.4$ and $z = 2.5$ were reported for polybutadiene gels[49] and polybutadiene gels,[50] respectively. For a PVC/dibutyl oxalate gel system, Lopez obtained $z = 3.7$.[51] The various gel systems show the different values of n, suggesting that n should be related to the gel structure. In this study, we found that $z = 3.0$ for both the hard gel and soft gel of F127, which is consistent with the prediction of the mean-field theory and is a typical characteristic for the gel formed by micelles packed into an ordered structure.

CONCLUSIONS

Multiple phase transitions and rheological scaling law for F127 aqueous solutions have been studied by a combination of micro-DSC and rheology. The thermoreversible micellization was observed in the process of heating and cooling, and the endothermic and exothermic curves displayed a mirror relationship for a given F127 concentration. The increase in F127 concentration resulted in the decrease in CMT. Beyond the primary peak for micellization, the second and third transition peaks were observed by micro-DSC for the concentrated aqueous solutions of F127 (higher than 20 wt %). These small peaks indicate the transitions of sol−gel and hard gel−soft gel, which was further confirmed by rheological measurements. The transition from the hard gel to the soft gel was considered to be due to the decrease in PEO block's solubility in the high temperature region, which resulted in the decrease in the entanglement density of PEO blocks. Using the Winter−Chambon criterion, the critical gel temperature T_{gel} has been obtained. A phase diagram, which could classify the regions for unimers, micelles, hard gel, and soft gel upon heating, has been determined. As F127 concentration increases, the critical relaxation exponent n decreased but the gel strength S_g increased. In the stable gel state, G_e showed the dependence on F127 concentration according to a scaling law, $G_e = 0.573c^{3.0}$ for the hard gel, and $G_e = 0.066c^{3.0}$ for the soft gel.

AUTHOR INFORMATION

Corresponding Author

*E-mail: mlli@ntu.edu.sg.

Notes

The authors declare no competing financial interest.

ACKNOWLEDGMENTS

This work was supported by the Academic Research Fund Tier 1 (2013-T1-002-072) from the Ministry of Education, Singapore.

REFERENCES

(1) Malmsten, M.; Lindman, B. Self-assembly in Aqueous Block Copolymer Solutions. *Macromolecules* **1992**, *25*, 5440−5445.

(2) Zhou, Z. K.; Chu, B. Phase Behavior and Association Properties of Poly(oxypropylene)−Poly(oxyethylene)−Poly(oxypropylene) Triblock Copolymer in Aqueous Solution. *Macromolecules* **1994**, *27*, 2025−2033.

(3) Alexandridis, P.; Olsson, U.; Lindman, B. Record of Nine Different Phases (Four Cubic, Two Hexagonal, and One Lamellar Lyotropic Liquid Crystalline and Two Micellar Solutions) in a Ternary

DOI: 10.1021/am507749w
ACS Appl. Mater. Interfaces 2015, 7, 2688−2697

Isothermal System of an Amphiphilic Block Copolymer and Selective Solvents (Water and Oil). *Langmuir* **1998**, *14*, 2627−2638.
(4) Bevan, M. A.; Scales, P. J. Solvent Quality Dependent Interactions and Phase Behavior of Polystyrene Particles with Physisorbed PEO−PPO−PEO. *Langmuir* **2002**, *18*, 1474−1484.
(5) Wu, C. J.; Schmidt, G. Thermosensitive and Dissolution Properties in Nanocomposite Polymer Hydrogels. *Macromol. Rapid Commun.* **2009**, *30*, 1492−1497.
(6) Alexandridis, P.; Athanassiou, V.; Fukuda, S.; Hatton, T. A. Surface Activity of Poly(ethylene oxide)-block-poly(propylene oxide)-block-poly(ethylene oxide) Copolymers. *Langmuir* **1994**, *10*, 2604−2612.
(7) Guo, C.; Wang, J.; Liu, H. Z.; Chen, J. Y. Hydration and Conformation of Temperature-Dependent Micellization of PEO−PPO−PEO Block Copolymers in Aqueous Solutions by FT-Raman. *Langmuir* **1999**, *15*, 2703−2708.
(8) Tsui, H. W.; Hsu, Y. H.; Wang, J. H.; Chen, L. J. Novel Behavior of Heat of Micellization of Pluronics F68 and F88 in Aqueous Solutions. *Langmuir* **2008**, *24*, 13858−13862.
(9) Alexandridis, P.; Nivaggioli, T.; Hatton, T. A. Temperature Effects on Structural Properties of Pluronic P104 and F108 PEO−PPO−PEO Block Copolymer Solutions. *Langmuir* **1995**, *11*, 1468−1476.
(10) Mortensen, K. Phase Behaviour of Poly(ethylene oxide)−Poly(propylene oxide)−Poly(ethylene oxide) Triblock Copolymer Dissolved in Water. *Europhys. Lett.* **1992**, *19*, 599−604.
(11) Kostko, A. F.; Harden, J. L.; McHugh, M. A. Dynamic Light Scattering Study of Concentrated Triblock Copolymer Micellar Solutions under Pressure. *Macromolecules* **2009**, *42*, 5328−5338.
(12) Wanka, G.; Hoffmann, H.; Ulbricht, W. Phase Diagrams and Aggregation Behavior of Poly(oxyethylene)−Poly(oxypropylene)−Poly(oxyethylene) Triblock Copolymers in Aqueous Solutions. *Macromolecules* **1994**, *27*, 4145−4159.
(13) Eiser, E.; Molino, F.; Porte, G.; Pithon, X. Flow in Micellar Cubic Crystals. *Rheol. Acta* **2000**, *39*, 201−208.
(14) Bahadur, P.; Li, P.; Almgren, M.; Brown, W. Effect of Potassium Fluoride on the Micellar Behavior of Pluronic F-68 in Aqueous Solution. *Langmuir* **1992**, *8*, 1903−1907.
(15) Jorgensen, E. B.; Hvidt, S.; Brown, W.; Schillen, K. Effects of Salts on the Micellization and Gelation of A Triblock Copolymer Studied by Rheology and Light Scattering. *Macromolecules* **1997**, *30*, 2355−2364.
(16) Li, H.; Yu, G. E.; Price, C.; Booth, C.; Hecht, E.; Hoffmann, H. Concentrated Aqueous Micellar Solutions of Diblock Copoly(oxyethylene/oxybutylene) E41B8: A Study of Phase Behavior. *Macromolecules* **1997**, *30*, 1347−1354.
(17) Dey, J.; Kumar, S.; Nath, S.; Ganguly, R.; Aswal, V. K.; Ismail, K. Additive Induced Core and Corona Specific Dehydration and Ensuing Growth and Interaction of Pluronic F127 Micelles. *J. Colloid Interface Sci.* **2014**, *415*, 95−102.
(18) Li, Y.; Shi, T.; Sun, Z.; An, L.; Huang, Q. Investigation of Sol−Gel Transition in Pluronic F127/D_2O Solutions Using a Combination of Small-Angle Neutron Scattering and Monte Carlo Simulation. *J. Phys. Chem. B* **2006**, *110*, 26424−26429.
(19) Mortensen, K.; Batsberg, W.; Hvid, S. Effects of PEO−PPO Diblock Impurities on the Cubic Structure of Aqueous PEO−PPO−PEO Pluronics Micelles: fee and bcc Ordered Structures in F127. *Macromolecules* **2008**, *41*, 1720−1727.
(20) Meznarich, N. A. K.; Love, B. J. The Kinetics of Gel Formation for PEO−PPO−PEO Triblock Copolymer Solutions and the Effects of Added Methylparaben. *Macromolecules* **2011**, *44*, 3548−3555.
(21) Desbrieres, J.; Hirrien, M.; Ross-Murphy, S. B. Thermogelation of Methylcellulose: Rheological Considerations. *Polymer* **2000**, *41*, 2451−2461.
(22) Lau, B. K.; Wang, Q.; Sun, W.; Li, L. Micellization to Gelation of a Triblock Copolymer in Water: Thermoreversibility and Scaling. *J. Polym. Sci., Part B: Polym. Phys.* **2004**, *42*, 2014−2025.
(23) Armstrong, J. K.; Chowdhry, B. Z.; Snowden, M. J.; Leharne, S. A. Effect of Sodium Chloride upon Micellization and Phase Separation Transitions in Aqueous Solutions of Triblock copolymers: A High-Sensitivity Differential Scanning Calorimetry Study. *Langmuir* **1998**, *14*, 2004−2010.
(24) Pham Trong, L. C.; Djabourov, M.; Ponton, A. Mechanisms of Micellization and Rheology of PEO−PPO−PEO Triblock Copolymers with Various Architectures. *J. Colloid Interface Sci.* **2008**, *328*, 278−287.
(25) Perreur, C.; Habas, J. P.; Peyrelasse, J.; Francois, J.; Lapp, A. Rheological and Small-Angle Neutron Scattering Studies of Aqueous Solutions of Branched PEO−PPO−PEO Copolymers. *Phys. Rev. E* **2001**, *63*, 0315051−03150511.
(26) Perreur, C.; Habas, J. P.; Lapp, A.; Peyrelasse, J. Salt Influence upon the Structure of Aqueous Solutions of Branched PEO−PPO−PEO Copolymers. *Polymer* **2006**, *47*, 841−848.
(27) Habas, J. P.; Pavie, M.; Lapp, A.; Peyrelasse, J. Understanding the Complex Rheological Behavior of PEO−PPO−PEO Copolymers in Aqueous Solution. *J. Rheol.* **2004**, *48*, 1−21.
(28) Almgren, M.; Brown, W.; Hvidt, S. Self-Aggregation and Phase Behavior of Poly(ethylene oxide)−Poly(propylene oxide)−Poly(ethylene oxide) Block Copolymer in Aqueous Solution. *Colloid Polym. Sci.* **1995**, *273*, 2−15.
(29) Habas, J. P.; Pavie, E.; Lapp, A.; Peyrelasse, J. Nonlinear Viscoelastic Properties of Ordered Phases of a Poly(ethylene oxide)−Poly(propylene oxide) Triblock Copolymer. *Rheol. Acta* **2008**, *47*, 765−776.
(30) Wang, Q.; Li, L.; Jiang, S. Effects of a PPO−PEO−PPO Triblock Copolymer on Micellization and Gelation of a PEO−PPO−PEO Triblock Copolymer in Aqueous Solution. *Langmuir* **2005**, *21*, 9068−9075.
(31) Li, L.; Lim, L. H.; Wang, Q.; Jiang, S. P. Thermoreversible Micellization and Gelation of A Blend of Pluronic Polymers. *Polymer* **2008**, *49*, 1952−1960.
(32) Shchipunov, Y. A.; Hoffmann, H. Indicative Evidence for Coexistence of Long and Short Polymer-like Micelles in Lecithin Organogel from Rheological Studies. *Langmuir* **1999**, *15*, 7108−7110.
(33) Feng, P.; Bu, X.; Pine, D. J. Control of Pore Sizes in Mesoporous Silica Templated by Liquid Crystals in Block Copolymer−Cosurfactant−Water Systems. *Langmuir* **2000**, *16*, 5304−5310.
(34) Kleitz, F.; Czuryszkiewicz, T.; Solovyov, L. A.; Linden, M. X-ray Structural Modeling and Gas Adsorption Analysis of Cagelike SBA-16 Silica Mesophases Prepared in A F127/Butanol/H_2O System. *Chem. Mater.* **2006**, *18*, 5070−5079.
(35) Winter, H. H.; Chambon, F. Analysis of Linear Viscoelasticity of A Crosslinking Polymer at the Gel Point. *J. Rheol.* **1986**, *30*, 367−382.
(36) Li, L.; Aoki, Y. Rheological Images of Poly(vinyl chloride) Gels. 1. The Dependence of Sol−Gel Transition on Concentation. *Macromolecules* **1997**, *30*, 7835−7841.
(37) Nijenhuis, K.; Winter, H. H. Mechanical Properties at the Gel Point of A Crystallizing Poly(vinyl chloride) Solution. *Macromolecules* **1989**, *22*, 411−414.
(38) Martin, J. E.; Adolf, D. The Sol−Gel Transition in Chemical Gels. *Annu. Rev. Phys. Chem.* **1991**, *42*, 311−339.
(39) Martin, J. E.; Adolf, D.; Wilcoxon, J. P. Viscoelasticity of Near-Critical Gels. *Phys. Rev. Lett.* **1988**, *61*, 2620−2623.
(40) Izuka, A.; Winter, H. H.; Hashimoto, T. Molecular Weight Dependence of Viscoelasticity of Polycaprolactone Critical Gels. *Macromolecules* **1992**, *25*, 2422−2428.
(41) Kjoniksen, A. L.; Nystrom, B. Effects of Polymer Concentration and Cross-Linking Density on Rheology of Chemically Cross-linked Poly(vinyl alcohol) Near the Gelation Threshold. *Macromolecules* **1996**, *29*, 5215−5222.
(42) Peyrelasse, J.; Lamarque, M.; Habas, J. P.; El Bounia, N. Rheology of Gelatin Solutions at the Sol−Gel Transition. *Phys. Rev.* **1996**, *53*, 6126−6133.
(43) Lu, A.; Wang, Y.; Boluk, Y. Investigation of the Scaling Law on Gelation of Oppositely Charged Nanocrystalline Cellulose and Polyelectrolyte. *Carbohydr. Polym.* **2014**, *105*, 214−221.

DOI: 10.1021/am507749w
ACS Appl. Mater. Interfaces 2015, 7, 2688−2697

(44) Scanlan, J. C.; Winter, H. H. Composition Dependence of the Viscoelasticity of End-Linked Poly(dimethylsiloxane) at the Gel Point. *Macromolecules* **1991**, *24*, 47−54.
(45) Li, L.; Aoki, Y. Rheological Images of Poly(vinyl chloride) Gels. 3. Elasticity Evolution and the Scaling Law beyond the Sol−Gel Transition. *Macromolecules* **1998**, *31*, 740−745.
(46) Gennes, P. G. D. *Scaling Concepts in Polymer Physics*; Cornell University Press: New York, 1979.
(47) Liu, S. J.; Yu, W.; Zhou, C. X. Solvents Effects in the Formation and Viscoelasticity of DBS Organogels. *Soft Matter* **2013**, *9*, 864−874.
(48) Flory, P. J. Molecular Size Distribution in Three Dimensional Polymers. I. Gelation. *J. Am. Chem. Soc.* **1941**, *63*, 3083−3090.
(49) Mours, M.; Winter, H. H. Relaxation Patterns of Nearly Critical Gels. *Macromolecules* **1996**, *29*, 7221−7229.
(50) Koike, A.; Nemoto, N.; Watanabe, Y.; Osaki, K. Dynamic Viscoelasticity and FT-IR Measurements of End-Crosslinking Dihydroxyl Polybutadiene Solutions Near the Gel Point in the Gelation Process. *Polym. J.* **1996**, *28*, 942−950.
(51) López, D.; Mijangos, C.; Muñoz, M. E.; Santamaría, A. Viscoelastic Properties of Thermoreversible Gels from Chemically Modified PVCs. *Macromolecules* **1996**, *29*, 7108−7115.

DOI: 10.1021/am507749w
ACS Appl. Mater. Interfaces 2015, 7, 2688−2697